Materials Science and Engineering R 73 (2012) 1–13

Contents lists available at SciVerse ScienceDirect

Materials Science and Engineering R

journal homepage: www.elsevier.com/locate/mser

Enhanced nanocatalysts

R.M. Mohamed [a,b,f], D.L. McKinney [c], W.M. Sigmund [d,e,*]

[a] Nanostructured Material Division Advanced Materials Department, Central Metallurgical R&D Institute, Helwan, 11421, Cairo, Egypt
[b] King AbdulAziz University, Faculty of Science, Chemistry Department, Advanced Materials, Nanocatalysis Group, Jeddah, 21589, Saudi Arabia
[c] MM Virtuoso, Inc. Gainesville, FL 32606, USA
[d] University of Florida, Department of Materials Science, Gainesville, FL 32611, USA
[e] Hanyang University, WCU Department of Energy Engineering, Seoul, South Korea
[f] Center of Excellence in Environmental Studies, King Abdulaziz University, P.O. Box 80216, Jeddah 21589, Saudi Arabia

ARTICLE INFO

Article history:
Available online 24 October 2011

Keywords:
Photooxidation
Nanocatalyst
Photoreduction
Semiconductor
Nanoparticles

ABSTRACT

Rapid development of nanofabrication techniques has created many different types of advanced nanosized semiconductors. Photocatalytic materials used to degrade organic and inorganic pollutants now include, in addition to TiO_2, ZnO, Fe_2O_3, WO_3, MoS_2, and CdS. Nanoparticles' unique properties, e.g. surface to volume ratio and quantum effects, continue to improve and expand photocatalysis' role in areas like environmental remediation, odor control, sterilization, and renewable energy. Controlling semiconductor size, shape, composition, and microstructure promises to benefit future research and applications in these fields. This review examines recent advances at the interface of nanoscience and photocatalysis, especially pertaining to nanocatalyst enhancements, for current and future environmental applications.

Published by Elsevier B.V.

Contents

* Corresponding author at: Hanyang University, WCU Department of Energy Engineering, Seoul, South Korea.
E-mail addresses: redama123@yahoo.com (R.M. Mohamed), sigmundmse@gmail.com (W.M. Sigmund).

0927-796X/$ – see front matter. Published by Elsevier B.V.
doi:10.1016/j.mser.2011.09.001

1. Introduction

As a pre-emptive caveat, for the most part, TiO_2 has been the material of choice for study as a nanocatalyst. As described in Section 2.3, it meets the photocatalytic semiconductor requirements. It is also useful in a variety of applications, and high quality samples are easily obtainable; furthermore, there has been a "self-promoting" popularity effect [1]. Therefore, it is natural that most of the studies reviewed here feature TiO_2 nanoclusters. The reader, though, is urged not to infer that this is the sole material possible to use. As mentioned in Section 5, though some has been done, more research is needed with other materials.

Air and water pollutants create significant environmental problems around the globe. Indeed, over the last decade, environmental pollution remediation became a national and global priority [2]. One promising technique for destroying contaminants is the application of photocatalysts [3]. Material development for photocatalysis evolved from conventional bulk metals and semiconductors to colloidal materials (~10–100 nm) to nanosized clusters (<10 nm) [4].

Stimulated by the oil crisis of the 1970s, interest in photocatalysis surged. The search for alternative energy sources led Fujishima and Honda to generate hydrogen by splitting water on a TiO_2 electrode (a photoelectrochemical cell) [5]. Anatase TiO_2 became the most widely investigated semiconductor in both alternative energy and environmental remediation research fields because of its availability, non-noxious nature, and photostability. Today, it is used to purify water and air, control odors, and sterilize [6].

Catalytic behavior is not only strongly materials-dependent, but also extremely size-dependent. Henglein showed that a nanomaterial can exhibit very different behavior compared to its bulk self [7,8]. Quantum confinement and surface phenomena based on particle size dominate material properties at the nano-level. Thus, nanoscience research allows scientists to alter and enhance a material's physical properties by controlling electronic energy levels via quantum size and surface effects [4].

Because of the critical importance of renewable/alternative energy and environmental remediation, photocatalysis and nanoscience's union have produced several reviews already. Henglein wrote two landmark reviews in 1988 and 1989 concerning the photophysical properties of nanosized semiconductors [7,8]. Gratzel followed up with a review on the photochemical properties of colloidal semiconductors in 1989 [9], and Hagfeldt helped him review photoredox reactions in nanocrystalline systems in 1995 [10]. Since 1995, others examined issues of quantum size effects, focused on nanomaterials' uses in environmental and energy applications, and explored the role nanoparticles play in photocatalysis [2,3,11–13]. Finally, in 2005, Abrams and Wilcoxon explored the effect of advances in the fields of nanoscience and photocatalysis especially regarding the interplay between quantum confinement and surface effects and the applications of MoS_2 [4].

In this article, we will review recent examples of nanocrystalline semiconductors used in photocatalysis and ways to enhance such nanocatalysts. In Section 2, we review key concepts and fundamentals of photocatalysis and nanoscience. The heart and soul of this review is Section 3, where we cover recent enhancements to nanocatalysts. In Section 4, we discuss current and future applications, followed by Section 5's challenges for nano and photocatalyst researchers to engage.

2. Fundamentals of photocatalysis and nanocatalysts

2.1. Introduction to photocatalysis

Several terms related to photocatalysis exist [3,14,15]. Photo-oxidation and photoreduction refers to initiation of oxidation and reduction reactions by light. Photosensitization is a form of photocatalysis. Charge separation in semiconductor nanoparticles occurs when light excites their bandgaps. Photogenerated electrons and holes are capable of oxidizing/reducing adsorbed substrates (Fig. 1A). Or, the nanoclusters promote a photocatalytic reaction by acting as mediators for the charge transfer between two adsorbed molecules (Fig. 1B). This process is extensively used in photoelectrochemistry and imaging science. In the first case, charge transfer at the semiconductor–electrolyte interface follows bandgap excitation of a semiconductor nanoparticle. In the second case, the semiconductor nanoparticle quenches the excited state by accepting an electron, and either transferring the charge to another substrate or generating photocurrent [16]. In either case, the semiconductor sensitizer remains, thus it is described as photocatalytic. Though photocatalysis technically refers to when a catalyst fully regenerates after a reaction, here we follow Abrams and Wilcoxon's example and discuss all above species as photocatalytic [4,17].

Several semiconductors can act as photocatalysts for light-induced chemical transformations because of their unique electronic structure, e.g. TiO_2, ZnO, Fe_2O_3, WO_3, and CdS. Such

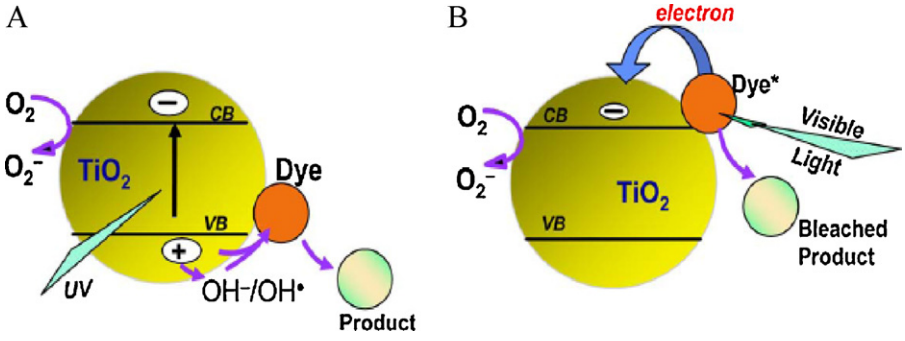

Fig. 1. Photoinduced charge-transfer processes in semiconductor nanoclusters. (A) Under bandgap excitation. (B) Sensitized charge injection by exciting adsorbed dye molecules. CB and VB refer to conduction bands and valence bands [16].
(Reproduced with permission from MATCHEMPHYS, Elsevier).

materials have a filled valence band and an empty conduction band. These semiconducting solids absorb photons (usually from UV illumination). When photon energy ($h\nu$) equals or exceeds the semiconductor's band gap, it excites an electron (e^-) from the valence band to the conduction band. It simultaneously generates an electron vacancy, a positive charge called a hole (h^+), in the valence band. Formulaically, this appears as follows:

$$h\nu + \text{semiconductor} \rightarrow h^+ + e^- \quad (1)$$

Then the semiconductor's electron transfers to an adsorbed compound. Put simply, the semiconductor oxidizes and the adsorbed compound reduces (Fig. 2).

The lifetime of an electron hole pair (e^-–h^+ pair) is but a few nanoseconds, yet that is still long enough to produce redox reactions in the solution or gas contacting the semiconductor [18]. Though other reactions of the migrated e^-–h^+ pair can occur (e.g., they recombine to produce thermal energy), generally the hole oxidizes water to hydroxyl radicals or combines with a donor specie's electron, and the electron gives itself to an acceptor molecule. When water is oxidized, subsequent reactions can then oxidize organic compounds. If the electron combines with an oxygen molecule, this forms superoxide radicals. When it combines with a metal ion, the ion can reduce to a lower valence state and deposit on the catalyst's surface. This electron-transfer process is more efficient if the species are preadsorbed on the surface.

2.2. Overview of photocatalysis as used in environmental remediation

2.2.1. Fundamental chemistry

Karakitsou and Verykios outlined a schematic to degrade organic water contaminants by photocatalysis [19]. They proposed the hydroxyl radical (OH^-) to be the primary oxidant in the photocatalytic system and suggested that four steps, all based on attack of OH^-, lead to detoxification. They follow:

(i) Photon energy greater than the band gap excites the catalyst and generates electrons and holes.

$$TiO_2 + h\nu \rightarrow e^- + h^+ \quad (2)$$

(ii) An organic molecule (R_1) adsorbs on the catalyst surface (R_{1ads}) via lattice oxygen (O_L^{2-}) at the surface.

$$O_L^{2-} + Ti^{IV} + H_2O \rightarrow O_LH^- + Ti^{IV}{-}OH^- \quad (3)$$

$$Ti^{IV} + H_2O \rightarrow Ti^{IV}{-}H_2O \quad (4)$$

$$\text{site} + R_1 \rightarrow R_{1ads} \quad (5)$$

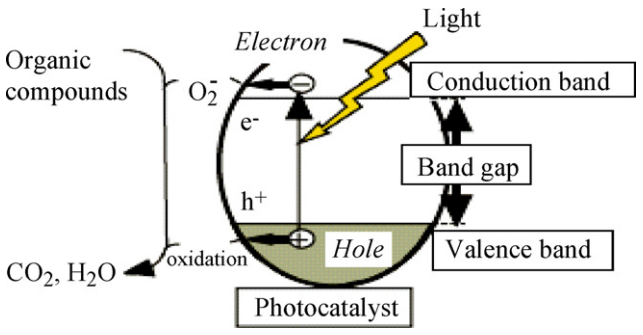

Fig. 2. Mechanism of photocatalysis: this diagram shows formation of holes (h^+) and electrons (e^-) upon irradiation of a semiconductor surface [200].
(Reproduced with permission from TitanPE Tech. (Shanghai) Inc. http://www.tipe.com.cn/library/kb2502.htm).

The e^-–h^+ pair recombines and produces thermal energy.

$$e^- + h^+ \rightarrow \text{heat} \quad (6)$$

The hole and electron become trapped.

$$Ti^{IV}{-}OH^- + h^+ \rightarrow Ti^{IV}{-}OH^{\bullet -} \quad (7)$$

$$Ti^{IV}{-}H_2O + h^+ \rightarrow Ti^{IV}{-}OH^{\bullet} + H^+ \quad (8)$$

$$R_{1ads} + h^+ \rightarrow R_{1ads}{}^+ \quad (9)$$

$$Ti^{IV} + e^- \rightarrow Ti^{III} \quad (10)$$

$$Ti^{III} + O_2 \rightarrow Ti^{IV}{-}O_2^{\bullet -} \quad (11)$$

Karakitsou and Verykios also proposed other cases where hydroxyl radicals, both adsorbed and free, can attack organic molecules, both adsorbed and free [19]. They follow:

$$\text{CaseI} : Ti^{IV}{-}OH^{\bullet} + R_{1ads} \rightarrow Ti^{IV} + R_{2ads} \quad (12)$$

$$\text{CaseII} : OH^{\bullet} + R_{1ads} \rightarrow R_{2ads} \quad (13)$$

$$\text{CaseIII} : Ti^{IV}{-}OH^{\bullet} + R_1 \rightarrow Ti^{IV} + R_2 \quad (14)$$

$$\text{CaseIV} : OH^{\bullet} + R_1 \rightarrow R_2 \quad (15)$$

In the case of other types of radicals, their reactions follow:

$$e^- + Ti^{IV}{-}O_2^{\bullet -} + 2H^+ \rightarrow Ti^{IV}(H_2O_2) \quad (16)$$

$$Ti^{IV}{-}O_2^{\bullet -} + H^+ \rightarrow Ti^{IV}(HO_2^{\bullet}) \quad (17)$$

$$H_2O_2 + OH^{\bullet} \rightarrow HO_2^{\bullet} + H_2O \quad (18)$$

Finally, an example of how electrons in the conduction band reduce metal ions (M^{n+}) follows [20]:

$$ne^- + M^{n+} \rightarrow M^0 \,(\text{ground state metal}) \quad (19)$$

2.2.2. Required semiconductor properties

Semiconductors used in photocatalysis need to possess certain characteristics. A photoanode's, or catalyst's, chemical make-up should be such that it can reverse its valence state to accommodate a hole without decomposing [21]. For example, in a non-stoichiometric TiO_2 reaction, $Ti^{3+} \rightarrow Ti^{4+}$. Also, the semiconductor's element needs to have more than one stable valence state. So, Cd^{2+} in CdS, or Zn^{2+} in ZnO, will not work because both decompose when holes form [22]. Other characteristics to consider when selecting a semiconductor include suitable band-gap energies [23], stability toward photocorrosion [21], nontoxic nature, stability under different reaction conditions [24,25], low cost, and physical characteristics that enable them to act as catalysts. TiO_2 meets all the above criteria, so it has been widely used in photoreactions [25]. However, other materials examined as potential photocatalysts to use against organic and inorganic pollutants include ZnO, ZrO_2, CdS, MoS_2, Fe_2O_3, WO_3, and various combinations [17,21,23–26].

2.3. Overview of nanocatalysts' material properties

The first account of light driven redox reactions in nanosystems was published in 1981 [12]. Since then, well studied nanocatalyst systems include oxides, sulphides and selenides: e.g., TiO_2, ZnO, WO_3, V_2O_5, Ag_2O, ZnS, CdS, PbS, Cu_2C, MoS_2, and CdSe [27–29]. And during the past decade, photochemistry of nanosized semiconductor particles has been one of the fastest growing research areas in physical chemistry [30]. This interest stems from the fact that nanosized semiconductor particles exhibit unique photophysical

and photocatalytic properties, distinct from their bulk counterparts [7,8,28,29,31]. They can possess enhanced photoredox chemistries and reduction reactions that might not otherwise occur using bulk materials [12].

The smaller a semiconductor particle becomes, the more the number of atoms located at the surface and the surface area to volume ratio increase [12,30]. This may enhance available surface-active sites and interfacial charge-carrier transfer rates, thus leading to higher catalytic activities [32]. One disadvantage does exist: only a smaller percentage of polychromatic light can be used, specifically higher energy light, for photocatalyst activation. The reasons are explained below.

Nanosized particles have diameters 1–10 nm, and clusters of nanosized particles (nanoclusters) exhibit transitional properties between molecular and bulk phases [31]. Thus, new terminology from quantum mechanics replaces some concepts in solid-state physics at the nano-level. For example, discrete densities of states displace band structure. In bulk materials, when light excites electrons, one finds them densely packed in the conduction band where they have varying kinetic energies [30]. Due to a nanoparticle's limited size, however, the conduction band's number of available states reduces. Thus, the generated e^-–h^+ pair only fits into such a particle when it assumes a higher kinetic energy state [33]. Such densities of states are now more specific, or discrete, unlike in the bulk material, where several energy levels may exist simultaneously.

2.3.1. Critical size and bandgap

The critical size for quantum effects of semiconductor particles seems to be when they are smaller than the Bohr radius of the first excitation state [27]. For example, TiO_2 has a critical diameter of 10 nm [11,34]. The electronic transitions of such particles in nanoclusters (nanocatalysts) behave more like molecules' highest occupied molecular orbitals (HOMOs) and lowest unoccupied molecular orbitals (LUMOs) [35]. For example, in gold and silver aqueous colloids, spatial-size confinement caused substantially slower electronic relaxation due to reduction of non-equilibrium electron transport and weaker electron–phonon coupling [36].

Moreover, as a result of the change in electronic properties, particle sizes also have a pronounced effect on semiconductor spectral properties [37]. Bahnemann et al. explained optical properties of semiconductor particles using the molecular orbital description [38]. During particle growth of TiO_2 particles from molecular to bulk sizes, molecular orbitals of an increasing number of molecules overlap, and the energy gap between the HOMO and LUMO decreases. Such changes result in a red shift (longer wavelength) of the accompanying optical transition [38]. Conversely, as particle size decreases, optical transition energy increases, i.e. fluorescent light color blue shifts [30].

Simply put, as particles become smaller, band gaps grow larger. Valence band levels moderately shift to lower energies, while conduction band levels strongly shift to higher energies [12]. And, the amount of necessary energy to excite electrons increases. Concurrently, more energy releases when the nanoparticles return to their resting states. Experiments on the change in the absorption spectrum of different materials verify this phenomenon. Fig. 3 illustrates particle size effects of CdS in aqueous solution. As particles become smaller, only higher energy wavelengths get absorbed. Similarly, Fig. 4 shows the absorption threshold as a function of particle size for CdS, ZnO, and PbS.

Mathematically, for a nanocatalyst, bandgap energy increase, ΔE_{BG}, varies with particle radius, R_{part}, reduced effective mass of excitation, μ, and semiconductor's dielectric constant, ε [39]. The following expression shows how μ relates to effective masses of charge carriers (m_e, m_h):

$$\mu^{-1} = m_e^{-1} + m_h^{-1}. \tag{20}$$

Finally, ΔE_{BG} depends critically on the effective masses of the electrons and holes [12]:

$$\Delta E_{BG} = \frac{h^2}{8\,\mu R_{part}^2} - \frac{1.8e^2}{\varepsilon R_{part}} \tag{21}$$

2.4. Determining optimally sized nanocatalysts

Some studies find that nanocatalysts exhibit enhanced photoactivity over their bulk-phase counterparts, and others do not [28]. As is now evident, particle size plays a determining role in

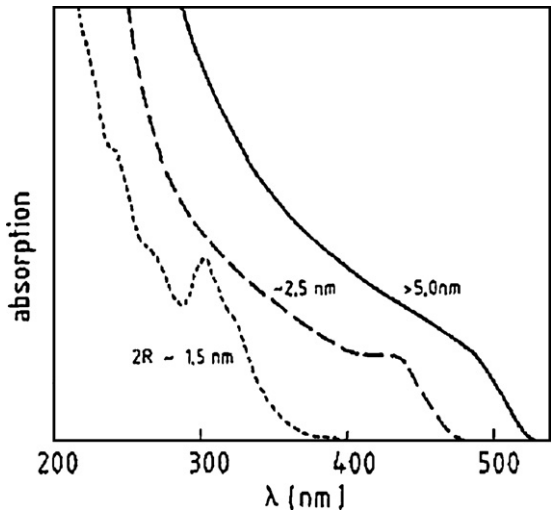

Fig. 3. Absorption spectrum of DcS in aqueous solution: different mean particle sizes [8].
(Reproduced with permission from Chemical Reviews, Copyright 1989 American Chemical Society.)

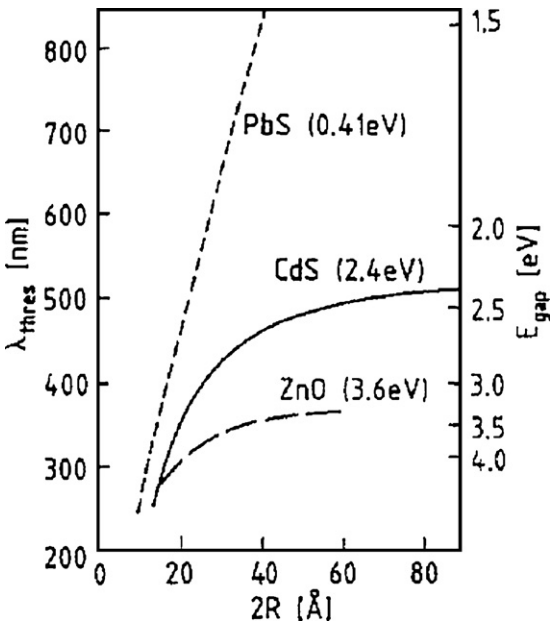

Fig. 4. Absorption threshold's wavelength as a function of CdS, ZnO, and PbS particle sizes. Right: band-gap energy. Gap energies of macrocrystalline materials given in parentheses [8].
(Reproduced with permission from Chemical Reviews, Copyright 1989 American Chemical Society.)

nanocluster activity. To achieve quantum electrical properties and spatial confinement of charge carriers in a TiO_2 system, for example, particles should have maximum diameter of ~10 nm. However, much smaller particles actually decrease photoactivity [40]. Zhang et al. explains why there is an optimally sized nanoparticle for nanocatalyst systems [41]. First, volume recombination of the charge carriers is the predominant process for larger particles. Decreased particle size reduces this effect, and it increases the surface area available for surface-active sites. Theoretically, it should also result in higher photonic efficiencies due to an increase in the interfacial charge-carrier transfer rates. However, as the particle size goes below a certain limit, surface recombination processes dominate: most e^-–h^+ pairs generate close to the surface, and surface recombination occurs faster than interfacial charge-carrier transfer processes. Thus, there exists an optimum particle size for maximum photocatalytic efficiency [41].

Since Abrams and Wilcoxon reviewed the research on how to produce nanoclusters in 2005, Liao and Liao showed that shape and size of TiO_2 nanoparticles can be controlled with surfactants [4,42]. They manipulated TiO_2 nanoparticles into spheres, cubes, ellipsoids, and nanorods using various surfactants. Cubic shaped and smaller-sized TiO_2 nanoparticles showed increased red shift in UV–vis light reflectance spectra. This lowers the required energy for photocatalysis and would be beneficial.

Two experiments in particular suggest that the optimal sized particle in TiO_2 nanocluster systems is 10–14 nm. Wang et al. studied chloroform decomposition. As particle size decreased from 21 to 11 nm, photoactivity efficiency improved. When particle size further decreased to just 6 nm, it worsened again. They suggested ~10 nm as the optimal size [40]. Koci et al. studied photocatalytic reduction of CO_2. Likewise, as they decreased particle sizes, they achieved higher yields of methanol and methane. But when they decreased particle size further, yields fell. The optimum particle size corresponding to the highest yields of both products was 14 nm [43]. Further study of optimal sizes for other nanocatalysts may improve applications.

3. Nanocatalyst enhancements

Photocatalysis promises to be a viable tool to remove vast quantities of undesirable chemical contaminants [39,44], but it can be made better. Succinctly put, the ensuing discussion centers around three fundamental approaches to enhancing photocatalytic activity: band-gap tuning and/or extension of excitation wavelength using photosensitizers, extending charge-carrier recombination times, and promoting forward reaction and reactant adsorbance by providing adequate quality and quantity of active sites [45].

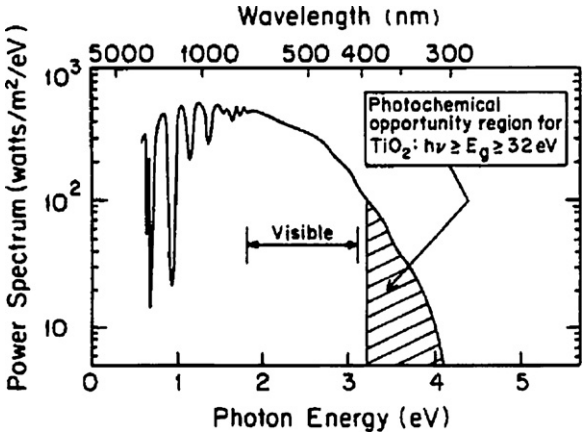

Fig. 5. Solar spectrum is at sea level with the sun at zenith; diagram shows the extremely limited absorption spectrum of unenhanced, bulk TiO_2 [3].
(Reprinted with permission from Chemical Reviews, Copyright 1995 American Chemical Society.)

Many TiO_2 nanocluster applications depend on the material's optical properties. Yet, highly efficient TiO_2 nanocatalyst use is sometimes thwarted because it has a wide band gap, which requires more energy. Fig. 5 shows that bulk TiO_2's band gap lies in the UV regime (3.0 eV for the rutile phase, 3.2 eV for the anatase phase), which is less than 10% of the sun's energy [3]. Thus, one goal to improve performance of TiO_2 nanocatalysts is to shift their onset of response from the UV to the visible region [46–48]. Nanoscience has helped do this.

There are several ways to achieve this goal, and this review article examines them. First, doping TiO_2 nanomaterials with other elements can narrow their electronic properties, thus altering TiO_2 nanomaterial's optical responses. Second, sensitizing TiO_2 with other colorful inorganic or organic compounds can improve its optical activity in the visible light region. Third, coupling collective oscillations of electrons in the conduction band of metallic nanoparticle surfaces to those in the conduction band of TiO_2 nanomaterials in metal–TiO_2 nanocomposites can improve performance. Finally, modifying TiO_2 nanocatalyst surfaces with other semiconductors can alter the charge-transfer properties between TiO_2 and the surrounding environment, thus improving the performance of TiO_2 nanomaterials-based devices.

3.1. Doping

Mills and Hoffman noted that doping a catalyst with a suitable material can enhance its performance [17]. Subsequently, Choi et al. systematically investigated metal ion doping in TiO_2 nanoclusters (2–4 nm) by measuring photoreactivity changes and transient charge-carrier recombination dynamics. They found that doped TiO_2 activity appeared to be a complex function of dopant concentration, dopant energy levels within the TiO_2 lattice, d electronic configuration, dopant distribution, electron donor concentration, and light intensity [49].

3.1.1. Metal ion doping

Since then, different metals have been doped into TiO_2 nanomaterials. Commonly assumed knowledge says that the noble metal ion acts as a sink for photoinduced charge carriers, and this promotes interfacial charge-transfer processes. Mills and Hoffman investigated by irradiating TiO_2 nanoparticles. The modified platinum or palladium outside the TiO_2 particles functioned as a "transient" anode. And they explained this phenomenon with the following oxidation reaction [17]:

$$Pt_0 + 2h^+ \rightarrow Pt^{2+} \quad (E_0 = 1.2\,V) \tag{22}$$

Indeed, selective metal ion doping of nanocrystalline TiO_2 does improve interfacial charge-transfer reactions [50]. Fig. 6 shows how the contact of metal with the semiconductor indirectly influences the energetic and interfacial charge-transfer processes favourably [16]. The metal ion traps the holes and electrons and prevents recombination of e^-–h^+ pairs. This helps maintain electroneutrality while degrading organic compounds.

Experimental proof of metal ion doping's enhancement abounds. To begin, Carraway et al., Cr-doped polycrystalline titania to use for N_2 photoreduction to NH_3 in the gas–solid regime and phenol photodegradation in the liquid–solid regime. Cr(III) ions improved charge separation of photoproduced e^-–h^+ pairs by means of a permanent electric field [26]. Choi et al. studied TiO_2 nanoparticles doped with metal ions via sol–gel and found that metal ion dopants significantly and positively influenced the photoreactivity, charge-carrier recombination rates, and interfacial electron-transfer rates

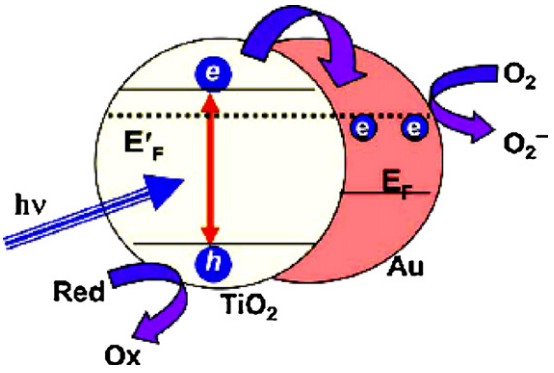

Fig. 6. Charge-transfer and Fermi-level equilibration in metal–semiconductor nanocomposites. E_F' and E_F refer to Fermi levels before and after equilibration [16]. (Reproduced with permission from MATCHEMPHYS, Elsevier.)

[51]. Li et al. developed La^{3+}-doped TiO_2 via sol–gel and found that lanthanum doping inhibits phase transformation of TiO_2, enhances its thermal stability, reduces its crystallite size, and increases Ti^{3+} surface content [52]. Nagaveni et al. prepared W-, V-, Ce-, Zr-, Fe-, and Cu-ion doped anatase TiO_2 nanoparticles via solution combustion and found that they limited solid formation within a narrow range of dopant ion concentrations [53]. Wang et al. prepared Nd^{3+}-doped and Fe(III)-doped TiO_2 nanoparticles with a hydrothermal method. They found that anatase, brookite, and trace hematite coexisted at lower pH levels (1.8 and 3.6) when Fe(III) content was as low as 0.5% even though Fe ion distribution was non-uniform between particles [40].

Continuing, Bessekhouad et al. investigated alkaline-doped (Li, Na, K) TiO_2 nanoparticles prepared via sol–gel and impregnation technologies and found that the crystalline levels were largely dependent on both the nature and the concentration of the alkaline. Li-doped TiO_2 produced the best crystallinity and K-doped TiO_2 the lowest [54]. Finally, Wang et al. synthesized Fe(III)-doped TiO_2 nanoparticles using oxidative pyrolysis of liquid-feed organometallic precursors in a radiation frequency (RF) thermal plasma and found that it strong promoted rutile formation (anatase phase is prevalent in non-doped TiO_2) [40].

Not all metal ion doping proves successful, though. Choi et al. prepared Sn^{4+}-doped TiO_2 nanoparticle films via the plasma enhanced CVD and discovered increased surface defects [51]. Gracia et al. synthesized M- (Cr, V, Fe, Co) doped TiO_2 nanoclusters via ion beam induced CVD and found that TiO_2 crystallized into either anatase or rutile structures, depending on the present cation's type and amount, with partial segregation of the cations in M_2O_n form after annealing [50].

3.1.2. Non-metal ion doping

Transition-metal ion doping and non-metal ion doping may extend TiO_2's response into the visible light region [55–59]. Various non-metal elements, C, N, S, F, Cl, and Br, have been successfully doped onto TiO_2 nanoclusters. The preparation methods of non-metal-doped TiO_2 nanomaterials can be divided into three types: wet chemistry, high temperature treatment, and ion implantation on TiO_2 nanomaterials. Wet chemistry methods usually involve hydrolysis of a titanium precursor in a mixture of water and other reagents, followed by heating.

To dope TiO_2 nanocatalysts with C, researchers used at least three different methods: heating titanium carbide, annealing TiO_2 under CO gas flow at high temperatures (500–800 °C), and directly burning a titanium metal sheet in a natural gas flame [60–64]. Similarly, several ways to dope TiO_2 nanomaterials with N include: hydrolyzing titanium tetraisopropoxide (TTIP) in a water/amine mixture and post-treating the TiO_2 sol with amines from a Ti-bipyridine complex, ball milling TiO_2 in a NH_3 water solution, heating TiO_2 under NH_3 flux at 500–600 °C, calcining the hydrolysis product of $Ti(SO_4)_2$ with ammonia as precipitator, decomposing gaseous $TiCl_4$ with an atmosphere microwave plasma torch, and sputtering/ion-implanting techniques with nitrogen [46–48,65–70].

In the same way, heat-induced reactions and sputtering/ion-implanting techniques can also dope S and F into TiO_2 nanoclusters. To synthesize S-doped TiO_2 nanocatalysts, scientists mixed TTIP with ethanol containing thiourea; heated sulphide powder; or used sputtering/ion-implanting techniques with S^+ ion flux [71,72]. F-doped TiO_2 nanomaterials were made by mixing TTIP with ethanol containing H_2O-NH_4F, heating TiO_2 under hydrogen fluoride, spray pyrolizing from an aqueous solution of H_2TiF_6, and using ion-implanting techniques with F^+ ion flux [52,67,73]. Finally, Liu et al. added $TiCl_4$ to HBr-containing ethanol to co-dope nanoclusters with Cl^- and Br [65].

It is important to note that changing doping methods may induce the dopants' different valence states. For example, incorporated S from thiourea induces S^{4+} or S^{6+} states, while direct heating of TiS_2 or sputtering with S^+ induces an S^{2-} anion [71,72]. Doping TiO_2 with cations of valences higher than the parent cation (Ti^{4+}) enhances H_2 production and photocatalytic efficiency [19]. Doping with ions of different valence states and the dopant's ability to change their valence state are important. These are directly related to the defects and their ability to contribute to the formation and or stabilization of the electron hole pair as well as increasing the transport properties for electrons, oxygen ions or holes to the surface.

3.2. Surface chemical modifications

Nanocatalyst efficiency depends, in part, upon the relative degree of reactive e^-–h^+ pairs branching into interfacial charge-transfer reactions. Because nanoclusters exhibit significantly increased surface to volume ratios, selectively treating particle surfaces can improve overall quantum efficiency of interfacial charge transfers [2]. Improving charge separation and inhibiting charge-carrier recombination is essential, and several approaches have been taken to achieve these goals: sensitizing semiconductor particles with redox couples or noble metals through surface chelation, derivatization, and platinization; simultaneous scavenging of holes and electrons by surface adsorbed redox species; and coupling semiconductor particles with different electronic energy levels [37,38,49,74–76].

3.2.1. Sensitization

TiO_2 is a semiconductor with a wide band gap; its optical absorption lies in the UV region (<400 nm). Any material with a narrower band gap, or absorption in infrared or visible light spectrums, can be used to sensitize TiO_2 materials. When light energy less than the semiconductor's band gap generates a photocurrent, the process is known as sensitization, and the light-absorbing dyes are referred to as sensitizers [31]. Such materials include inorganic semiconductors with narrow band gaps, metals, and organic dyes. How efficiently sensitized TiO_2 interacts with light largely depends on the sensitizer's light interaction characteristics, but other factors include efficient charge transfer from excited sensitizer to TiO_2 and the resultant charge separation, match between sensitizer's and TiO_2's electronic structures, and interface structures such as grain boundaries and bonding of the sensitizer and TiO_2. Careful design is needed to avoid charge trapping and recombination, which hampers sensitized TiO_2's performance [27].

3.2.1.1. Inorganic sensitization. Various groups have used narrow band gap semiconductors to improve optical absorption properties of TiO_2 nanoclusters in the visible light region over the past 15

years [52]. They usually prepare such inorganic semiconductor sensitized TiO_2 nanosystems via sol–gel method [77]. For example, Vogel et al. studied CdS, PbS, Ag_2S, Sb_2S_3, and Bi_2S_3 sensitized nanoporous TiO_2. At the inorganic nanoparticles and TiO_2 nanoparticles interface, they optimized energy levels for efficient charge separation using the size quantization effect. Also, they significantly enhanced TiO_2 electrodes' photostability by modifying their surfaces with CdS nanoparticles [78]. A year later, one of Vogel's coauthors, Hoyer, and Koenenkamp reported that they sensitized a TiO_2 nanocluster matrix with small PbS nanoparticles (<2.5 nm). They then directly injected the excess photogenerated electrons from PbS to TiO_2, and this resulted in strong photoconductivity in the visible light region [79]. That same year another research group, Fitzmaurice et al., discovered that exciting AgI sensitizers on TiO_2 nanoparticles resulted in stable e^-–h^+ pairs with a lifetime well beyond 100 μs and in electron migration from AgI to TiO_2 [80]. As pointed out above, increased charge transfer from sensitizer to TiO_2 factors into how efficiently sensitized TiO_2 interacts with light.

Just 10 years ago, Qian et al. used surface photovoltage spectra (SPS) measurements to prove that TiO_2 nanoparticles' large surface state density could be decreased by sensitization with CdS nanoparticles. Also, after CdS senisitization, they eliminated the TiO_2 nanofilm's slow photocurrent response and drastically increased its steady-state photocurrent [77]. Then, Sant and Kamat discovered that quantum size effects play an important role in interparticle electron transfer in CdS-TiO_2 semiconductor systems. Electron transfer from photoexcited CdS to TiO_2 depends on the TiO_2 nanoparticles' sizes. Charge transfer occurs only when TiO_2 nanoparticles are sufficiently large (>1.2 nm), so that TiO_2's conduction band is below that of CdS' [81]. Such information is useful to know for applications because it helps prevent resource and monetary waste.

In the same article, Sant and Kamat also sensitized mesoscopic TiO_2 films using bifunctional surface modifiers (SHR-COOH) linked with CdSe nanoparticles. Upon visible light excitation, CdSe nanoparticles injected electrons into TiO_2 nanocrystals. The TiO_2–CdSe composite exhibited a photon-to-charge-carrier generation efficiency of 12% when employed as a photoanode in a photoelectrochemical cell [81]. And most recently, Shen et al. studied differently sized TiO_2 nanoelectrodes sensitized with CdSe nanoparticles. They report that visible light region photoelectrochemical currents in CdSe-sensitized TiO_2 nanoclusters depend on both the TiO_2 electrode's structure and its electron diffusion coefficient [82].

3.2.1.2. Carbon nanotube sensitization. As it turns out, Schottky barriers more effectively increase recombination times for e^-–h^+ pairs. A Schottky barrier is a semiconductor–metal junction with a space-charge separation region. Where the two materials interface, electrons flow from one material to the other (from the higher to lower Fermi level) and align Fermi energy levels. With metals that have higher work function than the n-type semiconductor (e.g., TiO_2), electrons flow from the semiconductor to the metal. This Schottky barrier causes the metal to have excess negative charge, and the semiconductor to have excess positive charge. A depletion layer maintains charge separation in between the two. Traditionally, this method of extending recombination times was established with Pt and other noble metal interfaces [83].

Carbon nanotubes (CNTs) have a variety of electronic properties, including the ability to exhibit metallic conductivity as one of many possible electronic structures. CNTs have a large electron-storage capacity (one electron for every 32 carbon atoms) [84], therefore, they may accept photon-excited electrons in TiO_2 nanoclusters and thus retard or hinder e^-–h^+ pair recombination. Photon-generated e^-–h^+ pairs usually take about 10^{-9} s to recombine; however, Hoffman et al. measured chemical interactions with adsorbed pollutant species to take much longer, anywhere from 10^{-8} to 10^{-3} s [2]. A CNT–TiO_2 Schottky barrier effectively increases e^-–h^+ pair recombination time [16,83,85].

Further enhancements that CNTs provide include increased specific surface area and tailored specificity toward adsorbents through modification of the CNTs' surface groups. CNTs may also enhance photocatalytic efficiency by acting as a photosensitizer [86], thus extending TiO_2's photocatalytic ability into the visible spectrum [83,86,87].

Finally, CNTs solve two other problems that nanocatalysts have: difficulty distributing single particles, and collecting them after use. Support structures are needed for both. Two methods currently exist to attach CNT support matrices to TiO_2: electrospinning CNTs and TiO_2 nanofibers to yield mats with immobilized materials [88,89], and magnetizing Fe-filled CNTs in CNT–TiO_2 nanocomposites. Magnetic particles can then be dispersed with a magnetic fluidized bed [90].

For more details and examples of carbonaceous nanocatalyst enhancements, we refer the reader to Leary and Westwood's 2010 review [45]. They discuss activated carbon, carbon doping, carbon nanotubes [60], fullerenes, grapheme, thin layer carbon coating, nanometric carbon black, and others.

3.2.2. Coupling two semiconductor systems

Henglein et al. presented the first example in the literature of composite particles when he found that small amounts of Cd^{2+} added to ZnS quenched ZnS's bandgap fluorescence [8]. Nanophotosensitizers, such as CdS, and other nanomaterials not only extend TiO_2's spectral response into the visible region, but they also allow for interparticle electron transfer. ESR observed Ti^{3+} signal confirms electrons' vectorial displacement from nanophotosensitizers to TiO_2. Thus, coupling different semiconductor systems provides another way to improve charge-carrier separation, much like ion doping (see Section 3.1). Fig. 7 shows the charge-transfer processes involved in coupled semiconductor systems. Electrons photoinduced on the conduction band of a higher level semiconductor get injected into the lower level semiconductor's conduction band. As such coupled semiconductor systems offer great hope for advancing solar energy harvesting and environmental remediation techniques, governments and researchers dedicated considerable attention and resources to their synthesis, testing, and optimization [91–118].

First, organic–inorganic nanostructured composites emerged to generate a range of materials for catalytic technologies. In 1996,

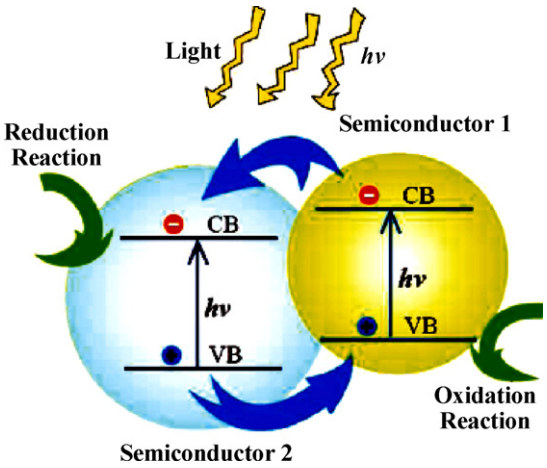

Fig. 7. Schematic illustration of charge transfer in a coupled semiconductor system [201].
(Reproduced with permission from Langmuir, Copyright 2010 American Chemical Society).

Braun et al. described the synthesis of stable semiconductor organic super lattices based on CdS and CdSe [119]. By incorporating organic molecules in an inorganic lattice, the authors anticipated that electronic properties could be tailored and that novel organic–inorganic composite nanostructures may be suitable for photocatalytic applications. Since then, successes worthy of note include research by Jang et al., who created a composite CdS-TiO_2 nanocatalyst that could degrade methylene blue under visible light illumination ($\lambda > 420$ nm) [120]. Tachibana et al. reported that photoelectrochemical solar cells based on very stable CdS sensitized TiO_2 nanoclusters exhibit high photocatalytic activity [121]. And, Yang et al. prepared ZnO–SnO_2 composite oxides with various molar ratios of Sn:Zn at different calcination temperatures via a facile cetyltrimethylammonium bromide (CTAB)-assisted co-precipitation method. Amorphous intermediates appear between evolutions of ZnO and SnO_2 crystals, and cubic ZnO–SnO_2 composite oxides (prepared with 2:1 Zn:Sn molar ratio at 700 °C calcination) exhibit the highest photocatalytic activity [92]. Sun et al. subsequently confirmed that Sn sensitizes ZnO; thus, this material pairing exhibits greater photocatalytic activity than ZnO alone [122].

Other coupled systems studied for their optical properties include ZrO_2–$TiO_{2-x}N_x$ [123], ZnS–CdS [124], CdS–Ag_2S [125–127], $Zn_xCd_{1-x}S$ and CdS–ZnS [128], AgI–Ag_2S [8,33], ZnS–CdSe [124], CdS–PbS [129], CdS–ZnO–CdO [130], ZnO–ZnS [131], ZnO–ZnSe [128], CdS–HgS [132], Ag–TiO_2–SiO_2 [102], and Pt–TiO_2–SiO_2 [91].

Heterogeneous semiconductor system development is very promising in other ways as well. By changing certain parameters, such as shell thickness or core particle radius, important photocatalytic, optical, and magnetic properties of nanocatalysts can be tailored. Also, problems like photodissolution, which might otherwise occur in 'unprotected' photocatalysts such as Fe_2O_3, can be addressed [12]. Another beneficial effect of foreign oxides is that they can greatly improve anti-sintering capability during heat-treatment. For example, ZrO_2 inhibits undesirable crystal growth during calcination when coupled with $TiO_{2-x}N_x$ nanoclusters. These composite nanocatalysts display higher porosity, higher specific surface area, and improved thermal stability over unmodified $TiO_{2-x}N_x$ samples. This proves beneficial for oxidizing gaseous organic compounds [123].

However, coupling semiconductors does not always enhance photocatalysis via charge separation. A coupled photocatalyst's design relies on its components' band structures. They are generally determined by many complex factors, including surface area, defect density, crystallinity, and quantum size effects. Also, in capped systems, if shell thickness is sufficiently thick relative to core radius, the two semiconductors retain their individual identity [76]. This means that only the holes are accessible at the nanocatalyst's surface. Though this does allow for selective interfacial charge transfer and improved oxidation efficiency, the reducing electrons are not utilized during the photocatalytic reaction (they are trapped within the core semiconductor). Therefore, such photocatalysts cannot be used for photoreduction or other reactions in which superoxide radicals (formed by the reduction of oxygen molecules) play a critical role.

Second, recently three-layered nanoparticles mark another development in surface-modified semiconductor nanoparticles. These nanoparticles consist of a quantum-sized core semiconductor particle, several layers of another semiconductor material covering it, and the core material finally deposited as the outermost shell. These particles are called quantum dots or wells [92], and the first example described in the literature was CdS–HgS–CdS [133]. Alternatively, a third material can also act as the outermost shell to enhance nanocatalysts. Experimentally, Lee et al. showed this to be true by preparing a hard, magnetic, triple composite nanocatalyst—BaFe-SiO_2-TiO_2 (magnetic core–intermediate layer–photoactive shell)—using wet-chemical methods. After heat-treatment, overall photocatalytic activity of the composite nanocatalyst improved [16]. Finally, Egypt's Central Metallurgical Research & Development Institute (CMRDI), alone and in cooperation with various U.S. institutions, works with many other three material composites to improve environmental pollutant degradation: V_2O_5–TiO_2–SiO_2 [93,107,108], ZnO–TiO_2–SiO_2 [107,108], V_2O_5–TiO_2–SiO_2, and Y_2O_3–Fe_2O_3–TiO_2 [93,95,98–100], Pt–Ti–HMS and Ag–Ti–HMS [91,101,103–106], Zn–TiO_2–ZnO [110], Ag–TiO_2–SiO_2 [102] and $BaCo_{0.5}Y_{0.5}O_3$ [112].

3.2.3. Nanocrystalline films and dye sensitization

Conventional powder nanocatalysts in colloid systems have limitations when they are used for environmental remediation. There is usually a need for post-treatment separation of byproducts to recover the nanocatalyst. To help overcome poor recyclability and tedious treatment, considerable research has been done to achieve immobilized semiconductor particles as thin films (nanocrystalline films) on a solid substrate. These can be traced back to the 1980s [133].

Nanocrystalline filmed materials are likely to find new industrial applications, such as antibacterial surfaces, and self-cleaning glass and ceramic tiles. Likewise, nanocrystalline films are of great importance for advanced photovoltaic devices and environmental pollutant sensors.

3.2.3.1. Films. Chemical vapor deposition or molecular beam epitaxy has been the preferred technique for depositing nanocrystalline films. Such films are comprised of a network conducive to electronic flow. Their nanoparticles are in electronic contact, allowing for electric charge percolation. This charge transport is highly efficient, and the quantum yield is practically unity [76]. Therefore, it is easy to manipulate photocatalytic processes via electrochemical methods. Fig. 8 illustrates how metal nanoparticles deposited on nanocrystalline TiO_2 films can enhance electrochemistry and photocatalysis.

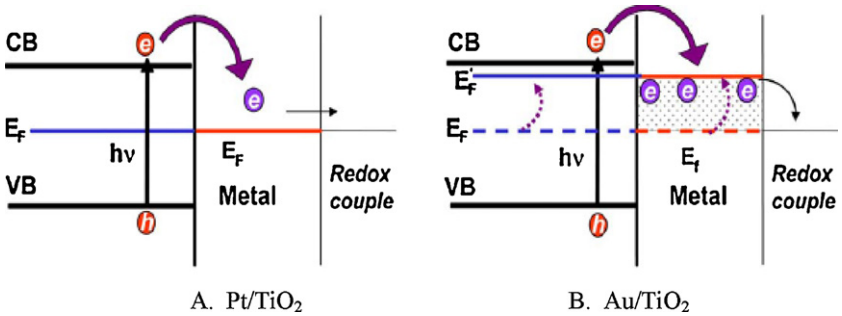

Fig. 8. This energy-level diagram illustrates the role of Pt (A) and Au (B) in dictating Fermi level equilibration of TiO_2–metal composite system [16]. (Reproduced with permission from MATCHEMPHYS, Elsevier.)

Another advantage is their high porosity. A conducting medium (electrolyte or other semiconductor) fills the pores between particles, forming junctions with extremely high surface area contact. This facilitates surface modifications with sensitizers, redox couples, and other semiconductors, which are highly beneficial in photocatalytic applications.

3.2.3.2. Dye sensitized films. Nanocrystalline films made from wide bandgap semiconductors, such as TiO_2, respond only in the UV region. Using dyes that strongly absorb in the visible light spectrum to sensitize the films is one way to extend their photoresponse. For example, in a porous nanocrystalline TiO_2 film, effective surface area can be 1000-fold more than in large colloidal particles. This makes light absorption ultra-efficient, even with a mere dye monolayer adsorbed on each particle [76].

3.2.3.3. Crystal facet engineering. We mentioned above that promoting forward reaction and reactant adsorbance by providing adequate quality and quantity of active sites is the third general direction that research has taken to enhance nanocatalyst performance [45]. And very recently, Liu et al. reviewed the literature with regard to this aspect. In 2011, they summarized the basic strategies for crystal facet engineering of photocatalysts, in particular TiO_2 crystals [134]. We refer the reader to their article for a detailed discussion on the history, basic synthesis strategies, crystal shape prediction, and photocatalytic activity of various synthesis parameters. Of interest, much of what they discuss intersects with the other directions of enhancement research, shown here in Fig. 9.

4. Nanocatalysts' applications

4.1. Introduction

It should be stressed that almost all environmental remediation and alternative energy research and advancements are closely linked to materials science and technology. In particular, nanoscience's contributions to photocatalysis have enabled us to select materials, enhance them, and tailor their properties to contaminants' specific chemistries for optimal photoreactions. No longer are we limited by bulk photocatalytic processes. Good research produces new knowledge, which enables new technologies. The nanocluster enhancements discussed so far are no exception. They were not discovered in a vacuum. Rather, usually each enhancement was paired and tested with a specific application in mind. This section highlights these applications.

4.2. Environmental remediation

Modern societies around the world face a critical problem: how to deal with environmental pollutants in our air and water. In the '80s and '90s, environmental pollution remediation became a high national and global priority [2]. Toxic waste pollutes rivers and lakes, tap water catches fire, and smog obscures many cities' otherwise impressive skylines. With increasing populations in developing countries, such phenomena will only get worse, unless science can address these problems with novel research, technologies, processes, and products. Throughout this review, it is mentioned that semiconductor photocatalysis offers one quantitative solution to the problem [44], and that nanocatalysts represent an advancement in this area. Indeed, complete mineralization of a wide variety of organic compounds has been reported [39], and last year, Teh and Mohamed reviewed published reports on advancements in photocatalytic degradation of organic pollutants in wastewater using TiO_2 [135]. Below in Table 1, we outline additional examples of reported environmental pollutants and their respective photocatalytic combatants. Together with those listed in Teh and Mohamed's review, these exemplify the range of applications, types of pollutants, and topics being researched, with novel ones continuously developing [136–138].

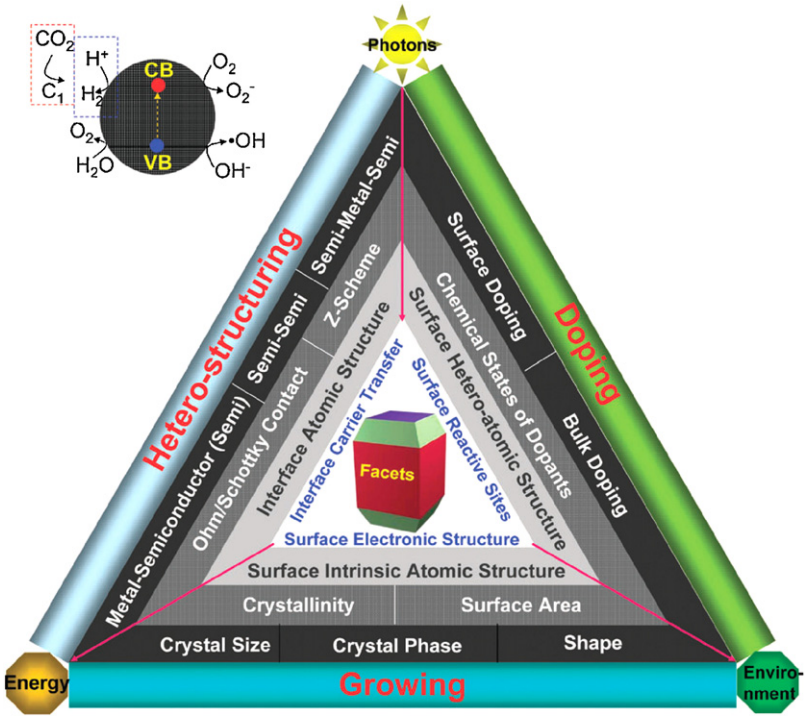

Fig. 9. This diagram illustrates the interrelationships between crystal structure, surface chemistry, and size of nanocatalysts [134]. (Reproduced with permission from Royal Society of Chemistry 2011.)

Table 1
Sample pollutants studied in past 20 years.

Pollutant	Nanocatalyst	Enhancement type	Success notes	Research group	Year
Phenol	TiO_2		After 120 h, no loss of catalyst	Schiavello [24]	1991
Phenol	TiO_2		No photocorrosion	Nair et al. [21]	1993
N_2	Cr(III) doped TiO_2	Ion doping	Improved charge separation of e^-–h^+ pairs	Carraway et al. [26]	1994
Phenol (C_6H_5OH)	Cr(III) doped TiO_2	Ion doping	Improved charge separation of e^-–h^+ pairs	Carraway et al. [26]	1994
Methyl orange	ZnO-SnO_2	Coupled systems	Cube morphology and Zn:Sn 2:1 ratio perform better	Yang et al. [92]	2010
CO_2	TiO_2		14 nm size yields most methanol and methane	Koci et al. [43]	2009
Orange II	TiO_2		Peptizer:TTIP 1:10 ratio performs better	Kim et al. [197]	2007
Mercury vapor	SiO_2-TiO_2	Coupled systems		Pitoniak et al. [147]	2005
Spores	TiO_2-multi-walled carbon nanotubes	CNTS, coupled systems	Effective against bioterrorism	Lee et al. [161]	2005
Organic azo dyes	TiO_2-BaFe	Coupled systems	Magnetized nanoparticles	Lee et al. [16,198]	2004, 2006
Methylene blue	CdS-TiO_2	Coupled systems	Used visible light, $\lambda > 420$ nm	Jang et al. [120]	2006
Gaseous organic compounds	ZrO_2-modified $TiO_{2-x}N_x$	Coupled systems	Inhibited undesirable crystal growth	Wang et al. [123]	2006
Isopropanol	TiO_2@SnO_2, SiO_2@TiO_2	Coupled/capped systems		Ohsaki et al. [199]	2006
Reactive black 5 Dye	ZnO film	Nanocrystalline films		Fouad et al. [95]	2005
Direct blue dye (DB53)	Ln doped TiO_2	Ion doping		El-Bahy et al. [96]	2009
CN^-, Phenol	TiO_2-SiO_2, V_2O_5-SiO_2	Coupled systems		Ismail et al. [98,99]	2003, 2004
Indigo carmine	Mn and La doped ZSM-5	Ion doping		Mohamed et al. [106]	2005
Indigo carmine	MnO_x-TiO_2	Coupled systems		Othman et al. [105]	2006
Cyanide, Cu(II)	TiO_2		Removed these contaminants from water	Barakat et al. [114]	2004
Phenol compounds	TiO_2-H_2O_2	Coupled systems		Fouad [107]	2007
2-chlorophenol	Co doped TiO_2 film	Ion doping, nanocrystalline films		Barakat et al. [116]	2004
Procion yellow H-EXL dye	TiO_2			Barakat [118]	2010

4.3. Noxious vapor control

Nanocatalysts can also be used to convert unwanted gaseous compounds into inert carbon dioxide and water. Gaseous toluene [139,140], formaldehyde [140], 1,3-butadiene [140], acetone [141–143], 1-butenol, butyraldehyde, formaldehyde, meta-xylene [141], ethylene [142–144], and others [145–147] have been studied. Because a photocatalyst can be reused, removal of noxious vapors using such a system is highly desirable in moderate and long-term applications, e.g. space shuttle cabins and the International Space Station [145].

An important consideration, in multi-gas experiments, compounds with lower affinity for the catalyst surface did not degrade until after higher affinity compounds were first catalysed [145]. This implies that in real world applications, nanocatalyst enhancements especially tailored to the targeted gas should be employed. If an environment generally has multiple problem gases, then multiple nanocatalyst systems will need to be employed simultaneously to ensure that no one gas builds up too much.

4.4. Bioparticle sterilization

Last year, Markowska-Szcupak et al. published a review, summarized here, that details TiO_2's role in killing bacteria, fungi, and other unwanted pathogenic organisms [148]. Matsunaga et al. first reported antimicrobial effects of TiO_2 photocatalysis in 1985 [149], and they continued to refine their processes to the point that $<1\%$ of *Escherichia coli* survived after just 16 min under irradiation [150]. Similar photocatalytic properties important for environmental remediation also appear to be important in antibacterial activity: surface area [151], particle size [151–154], and enhancing photocatalysts to perform well in the visible light spectrum [151,155–160]. Thus, continued improvement in nanocatalysts should also provide more effective antibacterial materials [151–162].

Interestingly, viruses appear to be the most photocatalytic-sensitive bioparticles studied [148]. Several studies show that TiO_2 effectively deactivates and destroys viruses [163–171]. Unfortunately, how the process works remains unclear [164]. Hence, more work must be done to determine which nanocatalyst enhancements are needed to improve antiviral properties.

Prions, fungi, and cancer also received attention from Markowska-Szcupak et al. [148]. One study showed successful prion destruction under UVA light [172]. Fungus destruction seems dependent on the species studied. More so than other bioparticles, fungi exhibit very diverse morphologies; each species reacts differently [149,173–182].

And nanoparticle TiO_2 anticancer applications might be the most exciting, yet least understood. Much work remains to be done in this area. Photocatalysis of cancer cells does seem promising; it most probably results in their apoptosis [183–190]. And in at least one instance, Illinois researchers proved they could kill brain cancer cells without hurting nearby normally healthy cells [189].

4.5. Renewable energy

4.5.1. Solar energy harvesting

Nanoscience has also helped improve solar cell energy production. Nanosized photosensitizers such as CdS not only extend the spectral response of TiO_2 into the visible region, but they also allow interparticle electron transfer. The Ti^{3+} signal observed by ESR confirms the vectorial displacement of electrons from CdS nanoclusters to TiO_2. Very recently, Tachibana et al. reported that photoelectrochemical solar cells based on very stable CdS nanocluster sensitized TiO_2 exhibit high photocatalytic activity. In addition, they investigated WO_3 as a potential photoanode for photoelectrochemical cells. Though they were stable against photocorrosion and absorbed a large portion of solar spectrum, their efficiency was still very low [121]. Such coupled semiconductor systems may well become important candidate materials for novel solar energy conversion devices.

4.5.2. H_2 production

In 1972, Fujishima and Honda achieved UV-light-induced water cleavage using a TiO_2 photoanode in combination with a Pt counter electrode soaked in an electrolyte aqueous solution [5]. Since then, semiconductor photocatalysis has attracted considerable attention as a method to generate hydrogen from water, and more recently, H_2S and other compounds [191]. H_2 could provide potential fuel for automotives, buildings, and even electronics, and photoelectrochemistry offers the cleanest way to produce it. TiO_2, MoS_2, and CdS are promising candidates for efficient H_2 production [28,126,192].

In 2006, Jang et al. coupled CdS nanoparticles with TiO_2 nanosheets to produce hydrogen. CdS helped sensitize TiO_2 and allowed hydrogen production in the visible light spectrum [120]. And just last year, Shen et al. reported that modifying the surfaces of platinized CdS powders with silver ions could activate these photocatalysts to produce H_2 as well [126]. Otherwise, CdS is inactive with respect to formation.

4.6. Polymerization

One final potential application that has not yet been addressed, or even mentioned beforehand, is the polymerization of various compounds. As with other nanophotocatalysis applications, this one marks a significant improvement over its bulk photocatalysis counterpart. Hoffmann et al. demonstrated in 1993 that bulk ZnO photoinitiators did not even polymerize the tested methyl methacrylate compound, whereas ZnO nanocatalysts did. Also, nanocluster CdS and TiO_2 semiconductors exhibited significantly higher yields than their bulk counterparts with respect to polymerization of several vinyl monomers [29].

5. Future challenges and concluding remarks

In some cases, learning from nature and living things may help us to design and create novel nanoarchitectures with both refined simplicity and beauty and mind-boggling complexity and detail. Within the field of semiconductor photocatalysis for environmental remediation, there is an urgent need to develop new photocatalytic materials that respond to sunlight by band structure control. This imperative will require researchers around the world to carry out systematic experimental studies and establish general design guidelines in band control engineering. Future work is also required to elucidate the mechanisms involved in the photocatalysis reactions. Our understanding of interfacial properties and charge transport in solar cells and sensing arrays for environmental monitoring will significantly benefit from advances in surface science and membrane-fabrication technologies.

In 2005, Abrams and Wilcoxon noted in their landmark review that TiO_2's drawbacks preclude its commercial use [4]. Thus, the search for new materials, development of other oxides, or ways to improve visible light absorption of materials through sensitization and band-gap manipulation via doping needs to continue so that nanoscience can provide new materials for viable photocatalysis.

One last concern is the possible impact nanoclusters may have on the environment and living organisms. Currently, little literature exists on concentration of nanoparticles in the environment and their potential influences. Chianelli et al. [193] and Colvin [194] discuss possible adverse affects, such as increased production of free radicals in the troposphere. And evidence exists that such nontoxic bulk material as TiO_2 can become toxic in nanoform [190,195,196]. Indeed, the International Agency for Research on Cancer (IARC) classified TiO_2 dust as an IARC Group 2B carcinogen.

The fusion of catalysis with nanotechnology continues to produce better materials and enhance their function. The recently discovered stability of graphene sheets and their use in photocatalysts is one of the latest examples. The new initiative in the United States to move materials more quickly from discovery and research into applications will surely find many material resources for market development of enhanced nanocatalysts.

Acknowledgements

This research was supported by WCU (World Class University) program through the Korea Science and Engineering Foundation (R31-2008-000-10092).

References

[1] U. Diebold, Surf. Sci. Rep. 48 (2003) 53–229.
[2] M.R. Hoffman, S.T. Martin, W. Choi, D.W. Bahnemann, Chem. Rev. 95 (1995) 69–96.
[3] A.L. Linsebigler, G. Lu, J.T. Yates, Chem. Rev. 95 (1995) 735–758.
[4] B.L. Abrams, J.P. Wilcoxon, Crit. Rev. Solid State Mater. Sci. 30 (2005) 153–182.
[5] A. Fujishima, K. Honda, Nature 238 (1972) 37–38.
[6] A. Fujishima, T.N. Rao, D.A. Tryk, Electrochim. Acta 45 (2000) 4683–4690.
[7] A. Henglein, Top. Curr. Chem. 143 (1988) 113–180.
[8] A. Henglein, Chem. Rev. 89 (1989) 1861–1873.
[9] M. Gratzel, in: N. Serpone, E. Pelizzetti (Eds.), Photocatalysis Fundamentals and Applications, John Wiley & Sons, New York, 1989, pp. 123–154.
[10] A. Hagfeldt, M. Gratzel, Chem. Rev. 95 (1995) 49–68.
[11] F.R. Howe, Dev. Chem. Eng. Mineral Process 6 (1998) 55.
[12] D. Beydoun, R. Amal, G. Low, S. McEvoy, J. Nanopart Res. 1 (1999) 439–458.
[13] B. Levy, J. Electrocer. 1 (1997) 239–272.
[14] N. Serpone, A.V. Emeline, Int. J. Photoener. 4 (2002) 91–131.
[15] H. Kisch, in: N. Serpone, E. Pelizzetti (Eds.), Photocatalysis Fundamentals and Applications, John Wiley & Sons, New York, 1989, pp. 1–8.
[16] S.W. Lee, J. Drwiega, C.Y. Wu, D. Mazyck, W.M. Sigmund, Mater. Chem. Phys. 96 (2006) 483–488.
[17] G. Mills, R.H. Hoffmann, Environ. Sci. Technol. 27 (1993) 1681–1689.
[18] K. Suzuki, in: D.F. Ollis, H. Al-Ekabi (Eds.), Photocatalytic Purification and Treatment of Water and Air, Elsevier, Amsterdam, 1993, p. 421.
[19] K.E. Karakitsou, E.X. Verykios, J. Phys. Chem. 97 (1993) 1184–1189.
[20] M. Gratzel, Acc. Chem. Res. 14 (1981) 376–384.
[21] M. Nair, H.Z. Luo, A. Heller, Ind. Eng. Chem. Res. 32 (1993) 2318–2323.
[22] A. Wold, Chem. Mater. 5 (1993) 280–283.
[23] M. Khan, N.N. Rao, J. Photochem. Photobiol. A 56 (1991) 101–111.
[24] M. Schiavello, Electrochim. Acta 38 (1993) 11–14.
[25] B.N. Jackson, M.C. Wang, Z. Luo, J. Schwitzgebel, J. Ekerdt, R.J. Brock, A. Heller, J. Electrochem. Soc. 138 (1991) 3660–3664.
[26] R.E. Carraway, A.J. Hoffman, M.R. Hoffmann, Environ. Sci. Technol. 28 (1994) 786–793.
[27] G.J. Highfield, P. Pichat, New J. Chem. 13 (1989) 61–66.
[28] M. Anpo, T. Shima, S. Kodama, Y. Kubokawa, J. Phys. Chem. 91 (1987) 4305–4310.
[29] A.J. Hoffman, H. Yee, G. Mills, M.R. Hoffmann, J. Phys. Chem. 96 (1992) 5540–5546.
[30] A. Henglein, Prog. Colloid Polym. Sci. 73 (1987) 1–3.
[31] W.D. Bahnemann, Isr. J. Chem. 33 (1993) 115–136.
[32] T.S. Martin, H. Herrmann, M.R. Hoffmann, J. Chem. Soc. Faraday Trans. 90 (1994) 3323–3330.
[33] H. Weller, A. Eychmüller, in: D.C. Neckers, D.H. Volman, G.V. Bünau (Eds.), Advances in Photochemistry, vol. 20, John Wiley & Sons, Hoboken, NJ, 1995 pp. 165–216.
[34] S. Martin, H. Herrmann, W. Choi, M. Hoffmann, J. Chem. Soc. Faraday Trans. 90 (1994) 3315–3322.
[35] L. Brus, J. Phys. Chem. 90 (1986) 2555–2560.
[36] A.B. Smith, D.M. Waters, A.E. Faulhaber, M.A. Kreger, T.W. Roberti, J.Z. Zhang, J. Sol. Gel. Sci. Technol. 9 (1997) 125–137.
[37] W.D. Bahnemann, A. Henglein, J. Lillie, L. Spanhel, J. Phys. Chem. 88 (1984) 709–711.
[38] W.D. Bahnemann, J. Monig, R. Chapmann, J. Phys. Chem. 91 (1987) 3782–3788.
[39] M.A. Fox, M.T. Dulay, Chem. Rev. 93 (1993) 341–357.
[40] Y. Wang, Y. Hao, H. Cheng, H. Ma, B. Xu, W. Li, W.S. Cai, J. Mater. Sci. 34 (1999) 2773–2779.
[41] Z. Zhang, C.C. Wang, R. Zakaria, J.Y. Ying, J. Phys. Chem. B 102 (1998) 10871–10878.
[42] D.L. Liao, B.Q. Liao, J. Photochem. Photobiol. A 187 (2007) 363–369.
[43] K. Koci, L. Obalova, L. Matejova, D. Placha, Z. Lacny, J. Jirkovsky, O. Solcova, Appl. Catal. B 89 (2009) 494–502.
[44] D.F. Ollis, H. Al-Ekabi (Eds.), Photocatalytic Purification and Treatment of Water and Air, Elsevier, Amsterdam, 1993, p. 3, Chap. 3.
[45] R. Leary, A. Westwood, Carbon 49 (2011) 741–772.
[46] C. Burda, Y. Lou, X. Chen, S.C.A. Samia, J. Stout, L.J. Gole, Nano Lett. 3 (2003) 1049–1051.
[47] X. Chen, C. Burda, J. Phys. Chem. B 108 (2004) 15446–15449.
[48] X. Chen, Y. Lou, S.C.A. Samia, C. Burda, L.J. Gole, Adv. Funct. Mater. 15 (2005) 41–49.

[49] W. Choi, A. Termin, R.M. Hoffmann, J. Phys. Chem. 98 (1994) 13669–13679.
[50] F. Gracia, P.J. Holgado, A. Caballero, R.A. Gonzalez-Elipe, J. Phys. Chem. B 108 (2004) 17466–17476.
[51] J.Y. Choi, A. Banerjee, A. Bandyopadhyay, S. Bose, in: S.W. Lu, M.Z. Hu, Y. Gogotsi (Eds.),Ceramic Nanomaterials and Technology III: Proceedings of the 106th Annual Meeting of the American Ceramic Society, Indianapolis, IN, USA 2004, Ceram. Trans. 159 (2005) 67–71.
[52] F.B. Li, X.Z. Li, F.M. Hou, Appl. Catal. B 48 (2004) 185–194.
[53] K. Nagaveni, M.S. Hegde, G. Madras, J. Phys. Chem. B 108 (2004) 20204–20212.
[54] Y. Bessekhouad, D. Robert, V.J. Weber, J.N. Chaoui, J. Photochem. Photobiol. A 167 (2004) 49–57.
[55] R. Asahi, T. Morikawa, T. Ohwaki, K. Aoki, Y. Taga, Science 293 (2001) 269–271.
[56] H. Irie, Y. Watanabe, K. Hashimoto, J. Phys. Chem. B 107 (2003) 5483–5486.
[57] G. Liu, N.Y. Zhao, H.C. Sun, F. Li, O.G. Lu, M.H. Cheng, Angew Chem. Int. Ed. 47 (2008) 4516–4520.
[58] D. Mitoraj, H. Kisch, Angew Chem. Int. Ed. 47 (2008) 9975–9978.
[59] S. Livraghi, C.M. Paganini, E. Giamello, A. Selloni, C. Di Valentin, G. Pacchioni, J. Am. Chem. Soc. 128 (2006) 15666–15671.
[60] G. Ma, X. Zhao, J. Zhu, Int. J. Mod. Phys. B 19 (2005) 2763–2768.
[61] V.D. Szabo, D. Vollath, W. Arnold, Ceram. Trans. 111 (2001) 217–224.
[62] S. Uchida, M. Tomiha, N. Masaki, A. Miyazawa, H. Takizawa, Sol. Energy Mater. Sol. Cells 81 (2004) 135–139.
[63] X. Wu, Z.Q. Jiang, F.Z. Ma, M. Fu, F.W. Shangguan, Solid State Commun. 136 (2005) 513–517.
[64] T. Yamamoto, Y. Wada, H. Yin, T. Sakata, H. Mori, S. Yanagida, Chem. Lett. 10 (2002) 964–965.
[65] Y. Liu, X. Chen, J. Li, C. Burda, Chemosphere 61 (2005) 11–18.
[66] M.S. Prokes, L.J. Gole, X. Chen, C. Burda, E.W. Carlos, Adv. Funct. Mater. 15 (2005) 161–167.
[67] H. Irie, Y. Watanabe, K. Hashimoto, J. Phys. Chem. B 107 (2003) 5483–5486.
[68] T.J. Chang, F.Y. Lai, L.J. He, Surf. Coat. Technol. 200 (2005) 1640–1644.
[69] O. Diwald, L.T. Thompson, T. Zubkov, E. Goralski, D.S. Walck, T.J. Yates, J. Phys. Chem. B 108 (2004) 6004–6008.
[70] C.Y. Hong, U.C. Bang, H.D. Shin, S.H. Uhm, Chem. Phys. Lett. 413 (2005) 454–457.
[71] T. Ohno, Water Sci. Technol. 49 (2004) 159–163.
[72] T. Umebayashi, T. Yamaki, S. Yamamoto, A. Miyashita, S. Tanaka, T. Sumita, K. Asai, J. Appl. Phys. 93 (2003) 5156–5160.
[73] G.J. Yu, C.J. Yu, B. Cheng, K.S. Hark, K. Iu, J. Solid State Chem. 174 (2003) 372–380.
[74] J. Moser, S. Punchihewa, P.P. Infelta, M. Gratzel, Langmuir 7 (1991) 3012–3018.
[75] P.A. Hong, W.D. Bahnemann, R.M. Hoffmann, J. Phys. Chem. 91 (1987) 2109–2117.
[76] I. Bedja, P.V. Kamat, J. Phys. Chem. 99 (1995) 9182–9188.
[77] X. Qian, D. Qin, Y. Bai, T. Li, X. Tang, E. Wang, S. Dong, J. Solid State Electrochem. 5 (2001) 562–567.
[78] R. Vogel, P. Hoyer, H. Weller, J. Phys. Chem. 98 (1994) 3183–3188.
[79] P. Hoyer, R. Könenkamp, Appl. Phys. Lett. 66 (1995) 349–351.
[80] D. Fitzmaurice, H. Frei, J. Rabani, J. Phys. Chem. 99 (1995) 9176–9181.
[81] A.P. Sant, V.P. Kamat, Phys. Chem. Chem. Phys. 4 (2002) 198–203.
[82] Q. Shen, D. Arae, T. Toyoda, J. Photochem. Photobiol. A 164 (2004) 75–80.
[83] K. Woan, G. Pyrgiotakis, W. Sigmund, Adv. Mater. 21 (2009) 2233–2239.
[84] A. Kongkanand, P.V. Kamat, ACS Nano 1 (2007) 13–21.
[85] J.L. Faria, W. Wang, in: P. Serp, J.L. Figueiredo (Eds.), Carbon Materials for Catalysis, John Wiley & Sons, Hoboken, NJ, 2009, pp. 481–506.
[86] W.D. Wang, P. Serp, P. Kalck, J.L. Faria, J. Mol. Catal. A: Chem. 235 (2005) 194–199.
[87] Y. Ou, J.D. Lin, S.M. Fang, D.W. Liao, Chem. Phys. Lett. 429 (2006) 199–203.
[88] S. Aryal, C.K. Kim, K.W. Kim, M.S. Khil, H.Y. Kim, Mater. Sci. Eng. C 28 (2008) 75–79.
[89] S.W. Lee, W.M. Sigmund, Chem. Commun. 6 (2003) 780–781.
[90] N. Grobert, W.K. Hsu, Y.Q. Zhu, J.P. Hare, H.W. Kroto, D.R.M. Walton, M. Terrones, H. Terrones, P. Redlich, M. Ruhle, R. Escudero, F. Morales, Appl. Phys. Lett. 75 (1999) 3363–3365.
[91] R.M. Mohamed, J. Mater. Process Tech. 209 (2009) 577–583.
[92] Z. Yang, L. Lv, Y. Dai, Z. Xv, D. Qian, Appl. Surf. Sci. 256 (2010) 2898–2902.
[93] A.A. Ismail, Preparation of titania-silica aerogel by sol-gel techniques for treatments of industrial waste waters, Ph.D. thesis, Faculty of Science, Ain Shams University, 2005.
[94] R.M. Mohamed, Preparation of vanadia-silica by sol-gel technique for industrial applications, MSc. Thesis, Faculty of Science, Ain Shams University, 2005.
[95] O.A. Fouad, A.A. Ismail, Z.I. Zaki, R.M. Mohamed, Appl. Catal. B 62 (2006) 144–149.
[96] Z.M. El-Bahy, A.A. Ismail, R.M. Mohamed, J. Hazard. Mater. 166 (2009) 138–143.
[97] W.L. Kostedt, A.A. Ismail, D.W. Mazyck, Ind. Eng. Chem. Res. 47 (2008) 1483–1487.
[98] A.A. Ismail, I.A. Ibrahim, M.S. Ahmed, R.M. Mohamed, H. El-Shall, J. Photochem. Photobiol. A 163 (2004) 445–451.
[99] A.A. Ismail, I.A. Ibrahim, R.M. Mohamed, Appl. Catal. B 45 (2003) 161–166.
[100] A.A. Ismail, Appl. Catal. B 85 (2008) 33–39.
[101] R.M. Mohamed, K. Mori, H. Yamashita, Int. J. Nanopart 2 (2009) 512–521.
[102] R.M. Mohamed, J. Alloys Compd. 501 (2010) 301–306.
[103] R.M. Mohamed, F.M. Ibrahim, K. Mori, H. Yamashita, in: A. Gédéon, P. Massiani, F. Babonneau (Eds.),Zeolites and Related Materials: Trends, Targets, and Challenges, Proceedings of the 4th International FEZA Conference, Paris, France, Elsevier, B.V., Stud. Surf. Sci. Catal. 174 (2008) 1255–1258.
[104] M.M. Mohamed, I. Othman, R.M. Mohamed, J. Photochem. Photobiol. A 191 (2007) 153–161.
[105] I. Othman, R.M. Mohamed, I.A. Ibrahim, M.M. Mohamed, Appl. Catal. A 229 (2006) 95–102.
[106] R.M. Mohamed, A.A. Ismail, I. Othman, I.A. Ibrahim, J. Mol. Catal. A: Chem. 238 (2005) 151–157.
[107] A.A. Ismail, U.S.-Egypt Joint S&T Project, Academy of Scientific Research and Technology, Ministry of Scientific Research, Final report: synthesis and characterization of TiO2-ZnO nanoparticles via sol gel technique for wastewater treatment, 2007.
[108] A.A. Ismail, U.S.-Egypt Joint S&T Project, Academy of Scientific Research and Technology, Ministry of Scientific Research, Final report: preparation of mixed oxides by sol-gel technique for removal of heavy metals and destruction of toxic compounds from industrial waste streams, 2005.
[109] R.M. Mohamed, A.A. El-Midany, I. Othman, Res. Chem. Intermed. 34 (2008) 629–639.
[110] A.A. Aal, M.A. Barakat, R.M. Mohamed, Appl. Surf. Sci. 254 (2008) 4577–4583.
[111] R.M. Mohamed, M.M. Mohamed, Appl. Catal. A 340 (2008) 16–24.
[112] R.M. Mohamed, K. Mori, T. Ochmichi, H. Yamashita, Int. J. Nanomanufact. 4 (2009) 257–266.
[113] I. Ahmed, U.S.-Egypt Joint S&T Project, Academy of Scientific Research and Technology, Ministry of Scientific Research, First report: magnetic nano-composite as photocatalyst prepared by the sol-gel technique for degradation of organic dyes, 2009.
[114] M.A. Barakat, Y.T. Chen, C.P. Huang, Appl. Catal. B 53 (2004) 13–20.
[115] M.A. Barakat, J.M. Tseng, C.P. Huang, Appl. Catal. B 59 (2005) 99–104.
[116] M.A. Barakat, H. Schaeffer, G. Hayes, S.I. Shah, J. Appl. Catal. B 57 (2004) 23–30.
[117] S. Buzby, M.A. Barakat, H. Schaeffer, G. Hayes, S.I. Shah, J. Vac. Sci. Technol., B: Microelectron Nanometer Struct. Process Meas. Phenom. 24 (2006) 1210–1214.
[118] M.A. Barakat, J. Hydro. Environ. Res. 5 (2011) 137–142.
[119] V.P. Braun, P. Osenar, S.I. Stupp, Nature 380 (1996) 325–328.
[120] S.J. Jang, H.S. Choi, H. Park, W. Choi, S.J. Lee, J. Nanosci. Nanotechnol. 6 (2006) 3642–3646.
[121] Y. Tachibana, Y.H. Akiyama, Y. Ohtsuka, T. Torimoto, S. Kuwabata, Chem. Lett. 36 (2007) 88–89.
[122] J.H. Sun, S.Y. Dong, J.L. Feng, X.J. Yin, X.C. Zhao, J. Mol. Catal. A: Chem. 335 (2011) 145–150.
[123] C.X. Wang, C.J. Yu, L.Y. Chen, L. Wu, Z.X. Fu, Environ. Sci. Technol. 40 (2006) 2369–2374.
[124] J.R. Heine, J. Rodriguez-Viejo, M.G. Bawendi, K.F. Jensen, J. Cryst. Growth 195 (1998) 564–568.
[125] J.S. Jang, C.J. Yu, C.H. Choi, S.M. Ji, E.S. Kim, J.S. Lee, J. Catal. 254 (2008) 144–155.
[126] S. Shen, L. Guo, X. Chen, F. Ren, S. Mao, Int. J. Hydrogen Energy 35 (2010) 7110–7115.
[127] R.K. Sharma, S.N. Sharma, A.C. Rastogi, Curr. Appl. Phys. 3 (2003) 257–262.
[128] Y.C. Wang, C. Böttcher, W.D. Bahnemann, K.J. Dohrmann, J. Nanopart. Res. 6 (2004) 119–122.
[129] K.S. Babu, T.R. Kumar, P. Haridoss, C. Vijayan, Talanta 66 (2005) 160–165.
[130] R.M. Navarro, F. del Valle, J.L.G. Fierro, Int. J. Hydrogen Energy 3 (2008) 4265–4273.
[131] G. Hota, S.B. Idage, K.C. Khilar, Colloids Surf. A 293 (2007) 5–12.
[132] D.J. Elliot, D.N. Furlong, F. Grieser, Colloids Surf. A 155 (1999) 101–110.
[133] A. Mews, A. Eychmuller, M. Giersig, D. Schooss, H. Weller, J. Phys. Chem. 98 (1994) 934–941.
[134] G. Liu, J.C. Yu, G.Q.M. Lu, H.M. Cheng, Chem. Commun. 47 (2011) 6763–6783.
[135] C.M. Teh, A.R. Mohamed, J. Alloys Compd. 509 (2011) 1648–1660.
[136] W.M. Sigmund, Abs. Papers Am. Chem. Soc. 229 (Part 1) (2005) U929.
[137] W.L. Kostedt, J. Drwiega, D.W. Mazyck, S.W. Lee, W. Sigmund, C.Y. Wu, P. Chadik, Environ. Sci. Technol. 39 (2005) 8052–8056.
[138] D. Mazyck, J. Drwiega, C.Y. Wu, P. Chadik, S. Lee, W. Sigmund, SAE 2004 Trans. J. Aerosp. (2005), Paper # 2004-01-2404.
[139] A.J. Maira, J.M. Coronado, V. Augugliaro, K.L. Yeung, J.C. Conesa, J. Soria, J. Catal. 202 (2001) 413–420.
[140] T.N. Obee, R.T. Brown, Environ. Sci. Technol. 29 (1995) 1223–1231.
[141] J. Peral, D.F. Ollis, J. Catal. 136 (1992) 554–565.
[142] M.L. Sauer, D.F. Ollis, J. Catal. 149 (1994) 81–91.
[143] M.E. Zorn, D.T. Tomkins, W.A. Zeltner, M.A. Anderson, Appl. Catal. B 23 (1999) 1–8.
[144] M.E. Zorn, D.T. Tomkins, W.A. Zeltner, M.A. Anderson, Environ. Sci. Technol. 34 (2000) 5206–5210.
[145] M.E. Zorn, Proceed. 13th Ann. WI Space Conf. (2003), Photocatalytic Oxidation of Gas-Phase Compounds in Confined Areas: Investigation of Multiple Component Systems, pp. 1–8.
[146] E. Pitoniak, C.Y. Wu, D. Londeree, D. Mazyck, J.C. Bonzongo, K. Powers, W. Sigmund, J. Nanopart Res. 5 (2003) 281–292.
[147] E. Pitoniak, C.Y. Wu, D.W. Mazyck, K.W. Powers, W. Sigmund, Environ. Sci. Technol. 39 (2005) 1269–1274.
[148] A. Markowska-Szcupak, K. Ulfig, A.W. Morawski, Catal. Today 169 (2011) 249–257.
[149] T. Matsunaga, R. Tomoda, T. Nakajima, H. Wake, FEMS Microbiol. Lett. 29 (1985) 211–214.
[150] T. Matsunaga, R. Tomoda, T. Nakajima, N. Nakamura, T. Komine, Appl. Environ. Microbiol. 54 (1988) 1330–1333.
[151] A.G. Rincon, C. Pulgarin, Appl. Catal. B 44 (2003) 263–284.
[152] J. Wang, Z. Ji, Z. Shui, X. Wang, N. Ding, H. Li, Adv. Mater. Res. 96 (2010) 99–104.
[153] V.S. Desai, M. Kowshik, Res. J. Microbiol. 4 (2009) 97–103.
[154] G.K. Prasad, G.S. Agarwal, B. Sigh, G.P. Rai, R. Vijayaraghavan, J. Hazard. Mater. 165 (2009) 506–510.

[155] A.W. Morawski, M. Janus, B. Tryba, M. Inagaki, K. Kalucki, CR Chim. 9 (2006) 800–805.
[156] M. Anpo, Pure Appl. Chem. 72 (2000) 1265–1270.
[157] S. Gelover, L.A. Gómez, K. Reyes, M.T. leal, Water Res. 40 (2006) 3274–3280.
[158] R. Van Grieken, J. Marugán, C. Sordo, C. Pablos, Catl. Today 144 (2009) 48–54.
[159] C. Văcăroiu, M. Enache, M. Gartner, G. Popescu, M. Anastasescu, A. Brezeanu, N. Todorova, T. Giannakopoulou, Ch. Trapalis, L. Dumitru, World J. Microbiol. Biotechnol. 15 (2009) 27–31.
[160] P. Wu, R. Xie, K. Imlay, J.K. Shang, Environ. Sci. Technol. 44 (2010) 6992–6997.
[161] S.H. Lee, S. Pumprueg, B. Moudgil, W. Sigmund, Colloids Surf. B 40 (2005) 93–98.
[162] G. Pyrgiotakis, W. Sigmund, in: W. Sigmund, H. El-Shall, D.O. Shah, B.M. Moudgil (Eds.), Particulate Systems in Nano and Biotechnologies, CRC Press, Boca Raton, FL, 2009, pp. 283–308.
[163] P. Hajkova, P. Spatenka, J. Horsky, I. Horska, A. Kolouch, Plasma Proc. Polym. 4 (2007) 397–401.
[164] R. Xu, X. Liu, P. Zhang, H. Ma, G. Liu, Z. Xia, Wuhan Univ. Technol. Mater. Sci. 22 (2007) 422–425.
[165] R.J. Watts, S. Kong, M.P. Orr, G.C. Miller, B.E. Henry, Water Res. 29 (1994) 95–100.
[166] J.C. Sjorgren, R. Sierka, Appl. Environ. Microbiol. 60 (1994) 344–347.
[167] Q. Li, M.A. Page, B.J. Mariñas, J.K. Shang, Environ. Sci. Technol. 42 (2008) 6148–6153.
[168] X. Sang, T.G. Phan, S. Sugihara, F. Yagyu, S. Okitsu, M. Maneekarn, W.E. Müller, H. Ushijima, Clin. Lab. 53 (2007) 413–421.
[169] C. Guillard, T.H. Bui, C. Felix, V. Moules, B. Lina, P. Lejeune, CR Chim. 11 (2008) 107–113.
[170] N.A. Mazurkowa, Y.E. Spitsyna, N.V. Shikina, Z.R. Ismagilov, S.N. Zagrebelnyi, E.I. Ryabchikova, Nanotechnol. Russ. 5 (2010) 417–420.
[171] K. Ulfig, in: J.K. Misra, S.K. Deshmuhk (Eds.), Fungi from Different Environments, Science Publishers, U.S., 2009, pp. 4–45.
[172] N. Psapltsis, K. Kotta, R. Lagoudaki, N. Grigoriadis, I. Poulios, T. Sklaviadis, J. Gen. Virol. 87 (2006) 3125–3130.
[173] D. Mitoraj, A. Jańczyk, M. Strus, H. Kirsch, G. Stochel, P.B. Heczko, W. Macyk, Photochem. Photobiol. Sci. 6 (2007) 642–648.
[174] K. Kühn, I.F. chaberny, K. Massholder, M. Stickler, V.W. Benz, H.G. Sonntag, L. Erdinger, Chemosphere 53 (2003) 71–77.
[175] N. Akiba, I. Hayakawa, E.S. Key, A. Watanebe, J. Med. Dent. Sci. 52 (2005) 223–227.
[176] O. Seven, B. Dindar, S. Aydemir, D. Metin, M.A. Ozinel, J. Photchem. Photobiol. A 165 (2004) 103–107.
[177] C. Maneerat, Y. Hayata, Int. J. Food Microbiol. 107 (2006) 99–103.
[178] J.S. Hur, A.O. Oh, K.M. Lim, J.S. Jung, J.W. Kim, Y.J. Koh, Postharvest. Biol. Technol. 35 (2004) 109–113.
[179] F. Chen, X. Yang, Q. Wu, Build Environ. 44 (2009) 1088–1093.
[180] C. Sichel, J. Tello, M. de Cara, P. Fernández-Ibáñez, Catal. Today 129 (2007) 152–160.
[181] C. Sichel, M. de Cara, J. Tello, J. Blanco, P. Fernández-Ibáñez, Appl. Catal. B 74 (2007) 152–160.
[182] L. Hochmannova, J. Vytrasova, Prog. Organic Coat. 67 (2010) 1–5.
[183] C. Guillard, J. Disdier, J.M. herrmann, C. Lehaut, T. Chopin, S. Malato, J. Blanco, Catal. Today 54 (1999) 217–228.
[184] H. Hidaka, S. Horikoshi, N. Serpone, J. Knowland, J. Photochem. Photobiol. A 111 (1997) 205–213.
[185] A.P. Zhang, Y.P. Sun, World J. Gastroenterol. 10 (2004) 3191–3193.
[186] A. Fujishima, R.X. Cai, J. Otsuki, K. Hashimoto, K. Itoh, T. Yamashita, Y. Kubota, Electrochim. Acta 38 (1993) 147–153.
[187] N. Lagopati, P.V. Kitsiou, A.I. Kontos, P. Venieratos, E. Kotsopoulou, A.G. Kontos, D.D. Dionysiou, S. Pispas, E.C. Tsilibary, J. Photochem. Photobiol. A 214 (2010) 215–223.
[188] L. Wang, J. Mao, G.H. Zhang, M.J. Tu, World J. Gastroenterol. 13 (2007) 4011–4414.
[189] E.A. Rozhkova, I. Ulasov, B. Lai, N.D. Dimitrijevic, M.S. Lesniak, T. Rajh, Nano Lett. 9 (2009) 3337–3342.
[190] Y. Chihara, K. Fujimoto, H. Kondo, Y. Moriwaka, T. Sasahira, Y. Hirao, H. Kyniyasu, Pathobiology 74 (2007) 353–358.
[191] S.A. Naman, S.M. Aliwi, K. Al-Emara, Int. J. Hydrogen Energy 11 (1986) 33–38.
[192] J.P. Wilcoxon, P.P. Newcomer, G.A. Samara, J. Appl. Phys. 81 (1997) 7934–7944.
[193] R.R. Chianelli, M.J. Yácaman, J. Arenas, F. Aldape, J. Hazard. Subst. Res. 1 (1998) 1–17.
[194] V.L. Colvin, Nat. Biotechnol. 21 (2003) 1166–1170.
[195] J.R. Gurr, A.S.S. Wang, C.H. Chen, K.Y. Jan, Toxicology 213 (2005) 66–73.
[196] R. Landsiedel, M.D. Kapp, M. Schulz, K. Wiench, Mutat. Res. 681 (2009) 241–258.
[197] J.H. Kim, W.Y. Jung, S.H. Baek, T.K. Lim, G.D. Lee, S.S. Park, S.S. Hong, Chem. Eng. Sci. 62 (2007) 5154–5159.
[198] S.W. Lee, J. Drwiega, C.Y. Wu, D. Mazyck, W.M. Sigmund, Chem. Mater. 16 (2004) 1160–1164.
[199] H. Ohsaki, N. Kanai, Y. Fukunaga, S.M. Watanabe, T.K. Hashimoto, Thin Solid Films 502 (2006) 138–142.
[200] Mechanism of photocatalysis, (Online) (Cited: July 20, 2011) http://www.tipe.com.cn/library/kb2502.htm.
[201] X. Hu, G. Li, J.C. Yu, Langmuir 26 (2010) 3031–3039.